Dynein light chain interaction with the peroxisomal import docking complex modulates peroxisome biogenesis in yeast

Jinlan Chang, Robert J. Tower, David L. Lancaster and Richard A. Rachubinski*

Department of Cell Biology, University of Alberta, Edmonton, Alberta T6G 2H7, Canada

*Author for correspondence (rick.rachubinski@ualberta.ca)

Accepted 12 July 2013
Journal of Cell Science 126, 4698–4706

doi: 10.1242/jcs.129056

Summary

Dynein is a large macromolecular motor complex that moves cargo along microtubules. A motor-independent role for the light chain of dynein, Dyn2p, in peroxisome biology in *Saccharomyces cerevisiae* was suggested from its interaction with Pex14p, a component of the peroxisomal matrix protein import docking complex. Here we show that cells of the yeast *Yarrowia lipolytica* deleted for the gene encoding the homologue of Dyn2p are impaired in peroxisome function and biogenesis. These cells exhibit compromised growth on medium containing oleic acid as the carbon source, the metabolism of which requires functional peroxisomes. Their peroxisomes have abnormal morphology, atypical matrix protein localization, and an absence of proteolytic processing of the matrix enzyme thiolase, which normally occurs upon its import into the peroxisome. We also show physical and genetic interactions between Dyn2p and members of the docking complex, particularly Pex17p. Together, our results demonstrate a role for Dyn2p in the assembly of functional peroxisomes and provide evidence that Dyn2p acts in cooperation with the peroxisomal matrix protein import docking complex to effect optimal matrix protein import.

Key words: Dynein, Peroxisome, *Yarrowia lipolytica*, Docking complex, Peroxin, Organelle biogenesis

Introduction

The molecular motor dynein has long been implicated in mitotic spindle positioning and the transport of organelles along microtubules (Kardon and Vale, 2009; Moore et al., 2009). Non-motor functions for components of dynein have been suggested by their interactions with proteins that have no evident link to subcellular motility (Fan et al., 1998; Navarro-Lérida et al., 2004). For example, dynein light chain, Dyn2p, was shown to help organize assembly of the nuclear pore complex in a motor-independent manner in the yeast *Saccharomyces cerevisiae* (Stelter et al., 2007). This study also reported that Dyn2p localized in part to peroxisomes through interaction with Pex14p, a component of the peroxisomal matrix protein import docking complex. Components of the dynein complex have also been shown to interact with Pex14 in human cells (Bharti et al., 2011), and a large-scale study of *S. cerevisiae* showed that cells deleted for the *DYN2* gene were unable to use oleic acid as a carbon source, the metabolism of which requires functional peroxisomes (Smith et al., 2006). Together, these findings suggest a role for Dyn2p in peroxisome biology.

Peroxisomes are ubiquitous membrane-bounded organelles involved in a variety of important biochemical and metabolic processes, notably the β-oxidation of fatty acids and the detoxification of reactive oxygen species (Fidaleo, 2010; Islinger et al., 2010). Peroxisomes also function as platforms for complex cellular signaling pathways such as those acting in antiviral innate immunity (Berg et al., 2012; Dixit et al., 2010; Horner et al., 2011). Several inborn human disorders are caused by peroxisome dysfunction. Patients with these disorders, collectively called the peroxisome biogenesis disorders, exhibit a variety of physiological abnormalities due to the absence of functional peroxisomes, and usually die within their first year (Fidaleo, 2010; Steinberg et al., 2006).

Peroxisomes arise by two different pathways: *de novo* biogenesis at the ER, and the growth and division of pre-existing peroxisomes (Ma et al., 2011; Mast et al., 2010; Schrader et al., 2012; Tabak et al., 2008). These two pathways work in concert to maintain the peroxisome population of a cell. Which pathway predominates depends on the type of cell and the internal and external environmental conditions to which it is exposed (Hoepfner et al., 2005; Kim et al., 2006; Motley and Hettema, 2007). The dynamic nature of peroxisome biogenesis leads to a heterogeneous population of peroxisomes at different stages of assembly (Titorenko and Rachubinski, 2000; Titorenko et al., 2000; van der Zand et al., 2012).

Proper import of peroxisomal matrix proteins is essential to peroxisome biogenesis. Peroxisomal matrix proteins are synthesized on cytosolic ribosomes and post-translationally imported into peroxisomes. Matrix proteins contain either a C-terminal peroxisome targeting signal type 1 (PTS1) or a PTS2 at or near their N-terminus (Gould et al., 1989; Swinkels et al., 1991). Translocation of matrix proteins across the peroxisomal membrane depends on the cycling receptors Pex5p and Pex7p (Marzioch et al., 1994; McCollum et al., 1993), which recognize PTS1- and PTS2-containing cargoes, respectively. Pex5p and Pex7p bind their cargo proteins in the cytosol and deliver them to

the peroxisome through interactions with the peroxisomal membrane proteins Pex13p, Pex14p and Pex17p, which make up the peroxisomal matrix protein import docking complex (Rucktäschel et al., 2011). Translocation of PTS1-containing proteins into the peroxisomal matrix is accomplished through a transient peroxisomal pore composed in part by Pex14p and cargo-laden Pex5p (Meinecke et al., 2010). The interaction of Dyn2p with Pex14p suggests a potential role for Dyn2p in matrix protein import into the peroxisome.

Here we show that absence of Dyn2p in the yeast *Yarrowia lipolytica* results in impaired peroxisome function and biogenesis, abnormal peroxisome morphology, and mislocalization of peroxisomal matrix proteins. We also demonstrate that Dyn2p physically and genetically interacts with docking complex proteins, suggesting that Dyn2p works in concert with the docking complex for efficient import of matrix proteins into the peroxisome.

Results

Dyn2p is required for normal peroxisome function and formation

The association of components of the dynein complex with peroxisomes in both yeast and mammalian cells and the demonstration that the dynein light chain protein, Dyn2p, interacts with the peroxisomal matrix protein import docking complex component Pex14p (Bharti et al., 2011; Stelter et al., 2007) suggest a possible role for components of dynein in peroxisome biogenesis. We chose to investigate the role of dynein light chain in peroxisome biogenesis using the heterothallic yeast *Yarrowia lipolytica* because of its robust growth and peroxisome proliferative capacity on medium containing fatty acid, the metabolism of which requires functional peroxisomes. A BLAST search of the *Y. lipolytica* proteome uncovered one homologue of *S. cerevisiae* Dyn2p: YALI0D07700p. *Y. lipolytica* Dyn2p exhibits 52% identity and 25% similarity to *S. cerevisiae* Dyn2p (Fig. 1A).

Deletion of the *DYN2* gene led to compromised growth of *Y. lipolytica* on oleic-acid-containing YPBO agar medium compared with that of the wild-type strain, although the growth defect was not as dramatic as that observed for cells deleted for the *PEX14* or *PEX17* gene encoding a component of the peroxisomal matrix protein import docking machinery (Fig. 1B). Transformation of the *dyn2*Δ strain with plasmid expressing the wild-type *DYN2* gene or a chimeric gene encoding fluorescent Dyn2p–mCherry re-established growth of the strain on YPBO, showing that the reduced ability of cells to grow on oleic-acid-containing medium was due specifically to deletion of the *DYN2* gene and that Dyn2p–mCherry functions similarly to Dyn2p (Fig. 1C). *Y. lipolytica* Dyn2p could also rescue the growth defect of a *S. cerevisiae* strain deleted for *DYN2* on oleic-acid-containing medium (supplementary material Fig. S1).

A reduced ability of *Y. lipolytica* to grow on oleic-acid-containing medium is often due to compromised peroxisome biogenesis, which in turn often results in abnormal peroxisome morphology. To see whether deletion of *DYN2* affects peroxisome biogenesis and/or morphology in *Y. lipolytica*, wild-type and *dyn2*Δ strains expressing the fluorescent PTS1-containing peroxisomal marker protein mRFP–SKL or the fluorescent PTS2-containing peroxisomal protein 3-ketoacyl-CoA thiolase tagged at its C-terminus with mRFP (Pot1p–mRFP) were cultured in glucose-containing YPD medium and

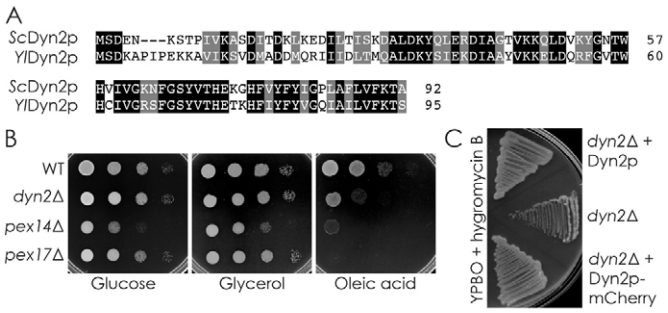

Fig. 1. Deletion of the *DYN2* gene impairs peroxisome function in *Y. lipolytica*. (A) Sequence alignment of *S. cerevisiae* Dyn2p with the putative Dyn2p homologue encoded by the open reading frame YALI0D07700 of the *Y. lipolytica* genome. Amino acid sequences were aligned using the ClustalW program (EMBL-EBI; http://www.ebi.ac.uk/Tools/msa/clustalw2). Identical residues are shaded black, and similar residues are shaded gray. Similarity rules: G=A=S; A=V; V=I=L=M; I=L=M=*F*=Y=W; K=R=H; D=E=Q=N; and S=T=Q=N. Dashes represent gaps. (B) *Y. lipolytica* deleted for the *DYN2* gene shows impaired growth on medium containing oleic acid, the metabolism of which requires functional peroxisomes. Growth of wild-type, *dyn2*Δ, and the peroxisome assembly mutant strains *pex14*Δ and *pex17*Δ on medium containing glucose (YPD), glycerol (YPG), or oleic acid (YPBO) as carbon source for 2 days at 30°C is shown. (C) Dyn2p and Dyn2p–mCherry rescue growth of the *dyn2*Δ strain on medium containing oleic acid. *DYN2* and *DYN2-mCherry* were expressed from the plasmid, pUB4. Empty pUB4 was introduced into the *dyn2*Δ strain as a negative control.

then transferred to oleic-acid-containing YPBO medium to promote peroxisome proliferation. Cells were observed by confocal microscopy at various times after transfer (Fig. 2A). With increasing time of incubation in YPBO medium, *dyn2*Δ cells exhibited localization of mRFP–SKL to discrete punctate structures similar to those observed in wild-type cells. Pot1p–mRFP also showed a punctate pattern of fluorescence in wild-type cells. Strikingly in contrast, Pot1p–mRFP in *dyn2*Δ cells showed predominantly a diffuse pattern of fluorescence characteristic of a cytosolic localization, although some fluorescent punctate structures were present. Therefore, fluorescence microscopy provides evidence of compromised matrix protein import in *dyn2*Δ cells.

The ultrastructure of peroxisomes in wild-type and *dyn2*Δ cells was compared by electron microscopy of cells incubated in YPBO medium for 10 hours (Fig. 2B). Wild-type cells showed typical round peroxisomes surrounded by a single unit membrane and containing a homogenous granular matrix. *dyn2*Δ cells occasionally contained peroxisomes similar to those seen in wild-type cells or large elongated peroxisomes (Fig. 2B,i) but usually contained small vesicular structures, some of which resembled peroxisomes (Fig. 2B,ii,iii). These vesicular structures were often observed arranged in tandem (Fig. 2B,ii) or clustered (Fig. 2B,iii). Together our data show that Dyn2p is required for normal peroxisomal matrix protein import and normal peroxisome function and formation under peroxisome proliferative conditions in oleic-acid-containing medium.

Peroxisomal matrix protein import and peroxisome maturation are impaired in *dyn2*Δ cells under conditions of peroxisome proliferation

One current model of peroxisome assembly in yeast proposes that peroxisomes are made *de novo* by the early fusion of distinct

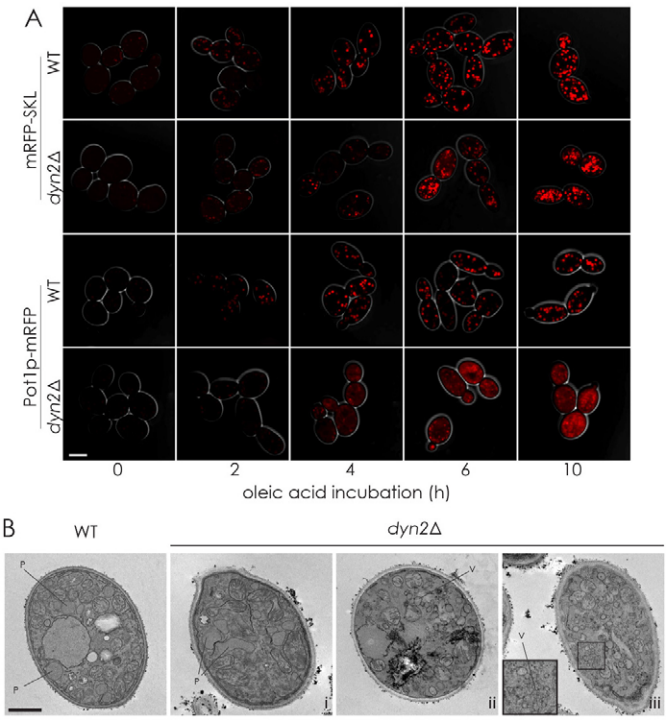

Fig. 2. Deletion of the *DYN2* gene affects peroxisomal matrix protein import and alters peroxisome morphology. (A) Wild-type and *dyn2*Δ cells were transformed with plasmids expressing the peroxisomally targeted fluorescent protein chimeras Pot1p-mRFP or mRFP-SKL. Transformed strains were grown in YPD medium, transferred to oleic-acid-containing YPBO medium, and imaged by fluorescence confocal microscopy at different times after transfer. Scale bar: 5 μm. (B) Ultrastructure of wild-type and *dyn2*Δ cells incubated in YPBO medium for 10 hours. P, peroxisome; V, vesicles. *dyn2*Δ cells lack peroxisomes or contain peroxisomes with abnormal profiles. Scale bar: 1 μm.

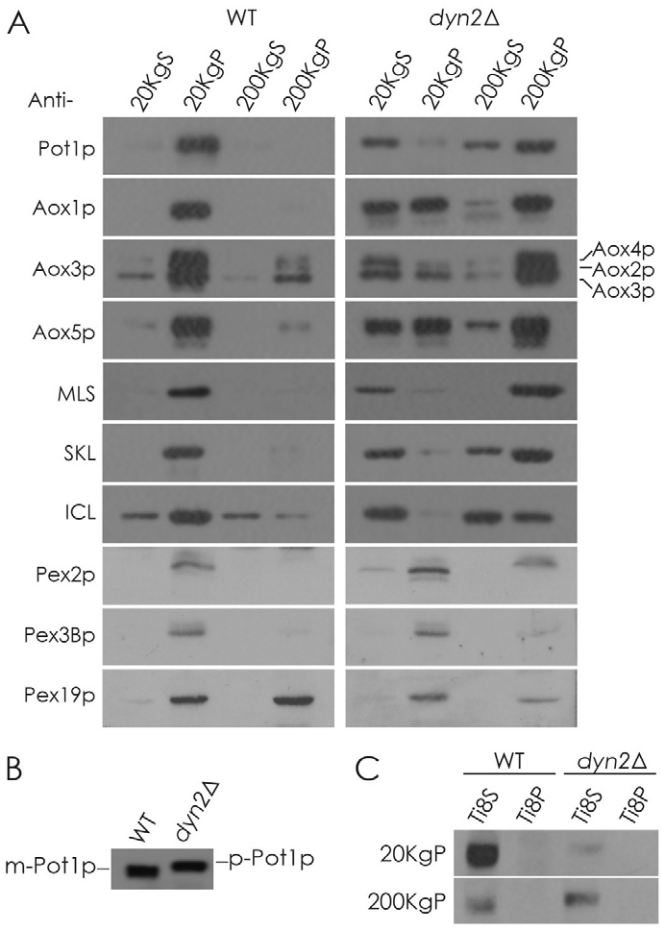

Fig. 3. Peroxisomal matrix proteins show altered localization in *dyn2*Δ cells incubated under peroxisome proliferating conditions. (A) Wild-type and *dyn2*Δ strains were cultured for 10 hours in oleic-acid-containing YPBO medium and subjected to subcellular fractionation to yield 20KgS, 20KgP, 200KgS and 200KgP fractions. One volume equivalents of the 20KgS and 200KgS fractions and 10 volume equivalents of the 20KgP and 200KgP fractions were analyzed by immunoblotting with antibodies to the indicated proteins. Anti-Aox3p antibodies recognize three isoforms of the enzyme fatty acyl-CoA oxidase, i.e. Aox2p, Aox3p and Aox4p. (B) Deletion of the *DYN2* gene prevents proteolytic processing of Pot1p to its mature form. 20KgP fractions from wild-type and *dyn2*Δ strains were analyzed by immunoblotting with anti-Pot1p antibodies. m-Pot1p, mature form of Pot1p; p-Pot1p, precursor form of Pot1p. (C) Translocation of Pot1p into the peroxisomal matrix is unaffected by deletion of the *DYN2* gene. 20KgP and 200KgP fractions from wild-type and *dyn2*Δ strains were treated with Ti8 buffer to lyse peroxisomes and then subjected to centrifugation to yield a supernatant fraction (Ti8S), enriched for soluble proteins, and a pellet fraction (Ti8P), enriched for membrane proteins. Equivalent portions of each fraction were analyzed by immunoblotting with anti-Pot1p antibodies.

peroxisomal precursors to produce another peroxisomal precursor that in turn is converted through the step-wise import of subsets of matrix proteins and phospholipids to eventually form a ‘mature’ peroxisome (Titorenko and Rachubinski, 2001; Titorenko et al., 2000; van der Zand et al., 2012). If matrix protein import along this pathway is compromised, peroxisome assembly and function are also usually compromised. In light of this link between peroxisome assembly/function and matrix protein import, and also considering the finding that Dyn2p co-purifies with the matrix protein import docking complex component, Pex14p (Stelter et al., 2007), we first examined matrix protein localization in *dyn2*Δ cells under conditions of peroxisome proliferation in oleic-acid-containing medium. Subcellular fractions from wild-type and *dyn2*Δ cells incubated in YPBO medium for 10 hours were subjected to immunoblot analysis for different matrix proteins, including the PTS1-containing proteins malate synthase (MLS) and isocitrate lyase (ICL); a 62-kDa protein reactive to antibodies against the tripeptide PTS1, Ser-Lys-Leu; the PTS2-containing protein Pot1p; and the five isoforms of the enzyme acyl-CoA oxidase (Aox1p to Aox5p), which contain neither a conventional PTS1 sequence nor a PTS2 sequence (Fig. 3A). As expected, matrix proteins in wild-type cells enriched primarily in the 20,000 ***g*** pellet (20KgP), which is enriched for ‘mature’ peroxisomes (Titorenko and Rachubinski, 2000; Titorenko et al., 2000). In contrast, matrix proteins in *dyn2*Δ cells were often observed across all fractions, with several enriched preferentially in the 200,000 ***g*** pellet (200KgP), which contains small peroxisomal vesicles (Titorenko and Rachubinski, 2000; Titorenko et al., 2000), and the 200,000 ***g*** supernatant (200KgS), which is enriched for cytosol. The peroxisomal membrane proteins Pex2p, Pex3Bp and Pex19p were found to be similarly enriched in the 20KgP and 200KgP fractions from both wild-type and *dyn2*Δ cells. These results indicate that under

peroxisome proliferating conditions in oleic-acid-containing medium, a fraction of individual matrix proteins is found in peroxisomes in *dyn2*Δ cells, but unlike in wild-type cells, different matrix proteins in *dyn2*Δ cells were enriched more in the 200KgP fraction containing small peroxisomal structures and less in the 20KgP fraction containing peroxisomes. Deletion of the *DYN2* gene apparently has no or little effect on the localization of peroxisomal membrane proteins.

Protease protection was performed to confirm that matrix protein import into membrane-enclosed peroxisomal structures is compromised in *dyn2*Δ cells (supplementary material Fig. S2). Postnuclear supernatant (PNS) fractions containing immature and mature peroxisomes and cytosol from wild-type and *dyn2*Δ cells were subjected to treatment with increasing amounts of trypsin and analyzed by immunoblotting with antibodies to different peroxisomal matrix proteins. Matrix proteins from *dyn2*Δ cells were preferentially degraded with trypsin. Taken altogether, our findings strongly support that peroxisome maturation and peroxisomal matrix protein import are compromised in *dyn2*Δ cells under peroxisome proliferative conditions in oleic-acid-containing medium.

Interestingly, we also observed a defect in the post-translational processing of Pot1p in *dyn2*Δ cells (Fig. 3B). Normally, the 45-kDa precursor of Pot1p (p-Pot1p) is translocated into the peroxisomal matrix where it is proteolytically processed to its mature 43-kDa form (m-Pot1p) (Szilard et al., 1995). In *dyn2*Δ cells, Pot1p remained in precursor form. The inability to proteolytically process Pot1p was not due simply to flawed Pot1p import in *dyn2*Δ cells, as Pot1p was found in both the 20KgP and 200KgP fractions containing peroxisomal structures from *dyn2*Δ cells (Fig. 3A,C). Furthermore, hypotonic lysis of the organelles in the 20KgP and 200KgP fractions with dilute alkaline Tris buffer followed by ultracentrifugation liberated Pot1p to the Ti8S fraction enriched for matrix proteins and not the Ti8P fraction enriched for membrane proteins of both wild-type and *dyn2*Δ cells (Fig. 3C). Therefore, Pot1p found in the matrix of peroxisomal structures in *dyn2*Δ cells is primarily in the precursor form, p-Pot1p.

The limited growth of the *dyn2*Δ strain on YPBO medium containing oleic acid (Fig. 1B) and the localization of a fraction of several peroxisomal matrix proteins to the 20KgP fraction (Fig. 3A) suggested that the *dyn2*Δ strain contains some functional peroxisomes. Isopycnic density gradient centrifugation of the 20KgP fractions from the wild-type and *dyn2*Δ strains and immunoblotting with antibodies to different matrix proteins showed several matrix proteins to be enriched in different fractions in extracts of the two cell types (Fig. 4). In wild-type cells, matrix proteins peaked in fractions 3 and 4, as observed previously (Szilard et al., 1995; Titorenko et al., 1996). Matrix proteins from *dyn2*Δ cells were also enriched in fractions 3 and 4, suggesting that *dyn2*Δ cells contain some membrane-enclosed structures that resemble biochemically wild-type peroxisomes with regard to their density and matrix protein composition. Matrix proteins from *dyn2*Δ cells were also substantially present in fractions of greater and lesser density than fractions 3 and 4. Interestingly, not all matrix proteins in *dyn2*Δ cells exhibited the same shift in distribution to other fractions. For example, in *dyn2*Δ cells there was a shift of MLS and the 62-kDa SKL-containing protein to fractions of higher density, whereas other matrix proteins such as Aox3p and Aox5p shifted to fractions of lower density. Consistent with the results of

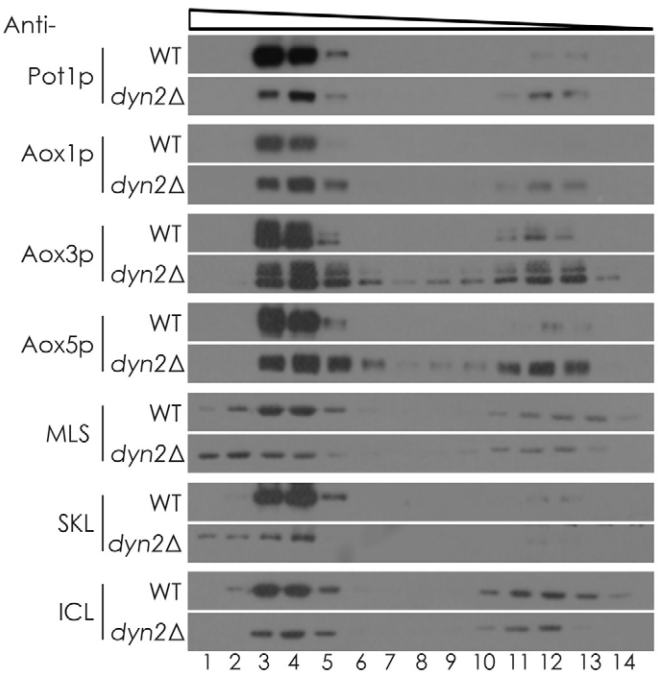

Fig. 4. Matrix proteins localize to different peroxisomal structures in *dyn2*Δ and wild-type cells incubated under peroxisome proliferating conditions. 20KgP fractions isolated from wild-type and *dyn2*Δ strains cultured for 10 hours in oleic-acid-containing YPBO medium were separated by isopycnic density gradient centrifugation on discontinuous Nycodenz gradients. Equal volumes of fractions were analyzed by immunoblotting with antibodies to the indicated proteins. Wedge depicts decreasing density of fractions.

fluorescence confocal microscopy and electron microscopy (Fig. 2), these data suggest that the peroxisome population of *dyn2*Δ cells is more heterogeneous in its composition than is the peroxisome population of wild-type cells. These findings are also consistent with previous observations that peroxisomal structures accumulate in yeast cells compromised in peroxisome biogenesis and that the matrix protein composition of these peroxisomal structures are different (Titorenko and Rachubinski, 2000; Titorenko et al., 2000; van der Zand et al., 2012).

We also compared matrix protein localization in wild-type and *dyn2*Δ cells incubated under peroxisome non-proliferating conditions in glucose-containing YPD medium. Immunoblot analysis showed that matrix proteins were distributed similarly in subcellular fractions from wild-type and *dyn2*Δ cells (supplementary material Fig. S3). The different peroxisomal matrix and membrane proteins were enriched preferentially in the 20KgP and 200KgP fractions from both wild-type and *dyn2*Δ cells. Our data suggest that *dyn2*Δ cells can import matrix proteins into peroxisomes as efficiently as wild-type cells under peroxisome non-proliferating conditions but are less efficient than wild-type cells when there is a demand for increased matrix protein import imposed by increases in peroxisome size and number under peroxisome proliferating conditions.

Dyn2p associates in part with peroxisomes *in vivo*

In *S. cerevisiae*, Dyn2p localization to the peroxisome is eliminated by deletion of the *PEX14* gene, and Pex14p is co-precipitated by Dyn2p in affinity purification (Stelter et al.,

2007). Using bimolecular fluorescence complementation (BiFC; also known as split GFP) (Munck et al., 2009), we showed that Dyn2p associates with Pex14p *in vivo* in *Y. lipolytica* (Fig. 5A). The N- and C-terminal-GFP-tagged constructs of Dyn2p and Pex14p were shown to function similarly to their wild-type counterparts as they were sufficient to restore growth of strains deleted for *DYN2* and *PEX14*, respectively, on oleic-acid-containing medium (supplementary material Fig. S4). The interaction of Dyn2p with Pex14p *in vivo* is independent of the import of most matrix proteins, as deletion of the gene *PEX5* encoding the PTS1 receptor did not eliminate the fluorescence resulting from interaction of the split GFPs fused to Dyn2p and Pex14p (Fig. 5A). In contrast, deletion of the *PEX17* gene encoding another component of the matrix protein import docking complex did eliminate the interaction between Dyn2p and Pex14p, suggesting that Pex17p helps to mediate the association between Dyn2p and Pex14p (Fig. 5A).

The association between Dyn2p and Pex14p occurred at the level of peroxisomes, as the GFP fluorescence resulting from Dyn2p interaction with Pex14p colocalized with the fluorescent peroxisomal marker, mRFP–SKL (Fig. 5B). Not all peroxisomes labeled with mRFP–SKL colocalized with the GFP signal, suggesting that Dyn2p may associate with a specific peroxisome subpopulation or that its interaction with peroxisomes is highly dynamic.

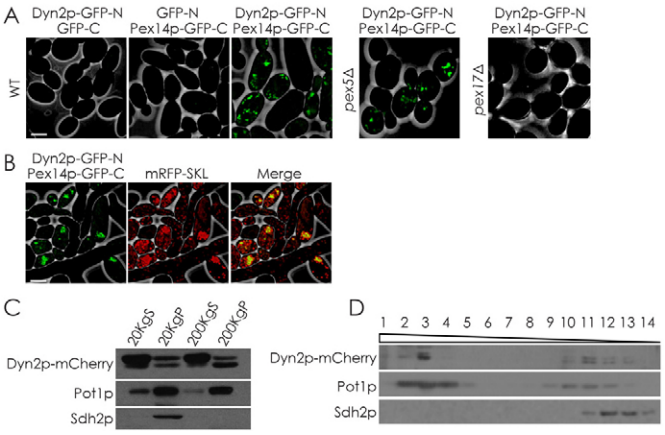

Fig. 5. Dyn2p interacts with the peroxisome docking complex protein, Pex14p, at the peroxisome. (A) Wild-type, *pex5*Δ and *pex17*Δ cells were transformed with plasmids expressing the N- or C-terminal half of GFP (GFP-N and GFP-C, respectively), Dyn2p fused at its C-terminus with GFP-N (Dyn2p–GFP-N), and Pex14p fused at its C-terminus with GFP-C (Pex14p–GFP-C) for analysis by BiFC, or split GFP, assay. Reconstitution of the GFP signal, as detected by fluorescence confocal microscopy, indicates interaction of the proteins. Scale bar: 5 µm. (B) Dyn2p and Pex14p interact at the peroxisome. Wild-type cells expressing Dyn2p–GFP-N, Pex14p–GFP-C and mRFP–SKL were cultured as in A and imaged by fluorescence confocal microscopy. Scale bar: 5 µm. (C) Dyn2p–mCherry localizes to the 20KgP fraction enriched for peroxisomes and the 200KgP fraction enriched for peroxisomal vesicles and other small vesicles. Cells expressing Dyn2p–mCherry were grown in YPD medium for 10 hours, and 20KgS, 20KgP, 200KgS and 200KgP fractions were prepared by subcellular fractionation. Equivalent portions of each fraction were analyzed by immunoblotting with antibodies to mCherry, the mitochondrial marker Sdh2p, and the peroxisomal marker, Pot1p. (D) Dyn2p–mCherry co-fractionates with peroxisomes. Organelles in the 20KgP fraction as in C were separated by isopycnic density gradient centrifugation on a discontinuous Nycodenz gradient. Equal volumes of fractions were analyzed by SDS-PAGE. Fractions enriched for peroxisomes and mitochondria were identified by immunodetection of Pot1p and Sdh2p, respectively. Wedge depicts decreasing density of fractions.

The *in vivo* detection of association between Dyn2p and Pex14p at the peroxisome predicts that some Dyn2p would co-purify with peroxisomes isolated by subcellular fractionation. As expected, a significant fraction of Dyn2p–mCherry localized to the 200KgS fraction enriched for cytosolic proteins (Fig. 5C). However, Dyn2p–mCherry was also found in the 20KgP fraction enriched for peroxisomes and mitochondria and in the 200KgP fraction enriched for small vesicles, including small peroxisomal vesicles (Fig. 5C). Interestingly, Dyn2p–mCherry migrates as a doublet in all fractions, with the lower molecular mass species most enriched in the 200KgP fraction. The origin and significance of this Dyn2p doublet are unknown but could be the result of a post-translational modification of Dyn2p, as has been reported for human dynein light chain 1 (Song et al., 2008), which could, for example, promote the association of Dyn2p with peroxisomes or peroxisomal vesicles. Isopycnic density gradient centrifugation of the 20KgP fraction indicated that Dyn2p–mCherry co-enriched with the peroxisomal matrix enzyme Pot1p but not with the mitochondrial protein Sdh2p (Fig. 5D), indicating that a portion of the Dyn2p localizes to peroxisomes.

Dyn2p interacts with the peroxisomal matrix protein import docking complex

We performed GST pull-down assays to differentiate between direct and bridged protein interactions with Dyn2p (Fig. 6A). GST alone, or GST fusions to Dyn2p and to the peroxisomal matrix protein import docking components Pex14p and Pex17p, immobilized on glutathione–Sepharose beads were used as bait for maltose binding protein (MBP) or MBP fusions to Dyn2p, Pex14p and Pex17p. MBP fusions were detected by immunoblotting with anti-MBP antibody. Expression of a MBP fusion to the docking complex protein Pex13p failed because of its cytotoxicity to *Escherichia coli*. Direct interaction was observed between Pex14p and Pex17p and between Pex14p and itself. GST–Dyn2p pulled down MBP–Dyn2p, MBP–Pex14p and MBP–Pex17p but not MBP alone. The interaction of GST–Dyn2p with MBP–Pex17p was particularly robust, suggesting that the interaction of Dyn2p with the peroxisomal matrix protein import complex is chiefly mediated through Pex17p.

The amino acid sequence VDAQTQTE (residues 99–106) of Pex17p is similar to putative Dyn2p-binding sequences found in dynein intermediate chain and Nup159p (Stelter et al., 2007; Stuchell-Brereton et al., 2011). We investigated whether V99DAQTQTE106 mediates the interaction of Pex17p with Dyn2p by constructing a series of MBP-tagged Pex17p mutants and truncations to act as potential binding partners for GST–Dyn2p and GST–Pex14p in GST pull-down assays (Fig. 6B,C). We found that mutation or deletion of the putative Dyn2p binding domain V99DAQTQTE106 of Pex17p eliminated the interaction between Pex17p and Dyn2p. This domain was not required for Pex17p to interact with Pex14p. However, deletion of the C-terminus of Pex17p eliminates the interaction of Pex17p with Pex14p, suggesting that the C-terminus of Pex17p is required for its interaction with Pex14p.

We next investigated the functionality of the mutants Pex17pΔ102–106 and Pex17p*mut* by evaluating their ability to complement the growth defect of *pex17*Δ cells on oleic-acid-containing YPBO medium (Fig. 7A). As expected, reintroduction of the *PEX17* gene restored growth of the *pex17*Δ strain on

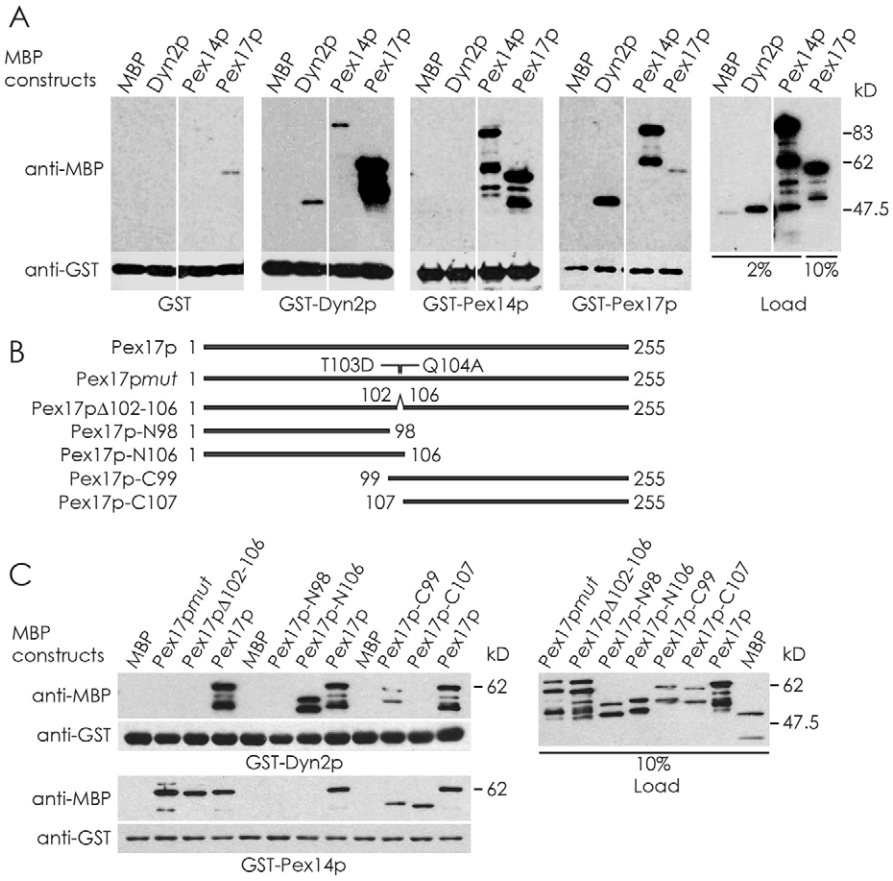

Fig. 6. Dyn2p interacts *in vitro* with the peroxisomal docking complex proteins Pex14p and Pex17p. (A) Glutathione–Sepharose beads containing GST alone or GST fused to Dyn2p, Pex14p, or Pex17p were incubated with extracts of *E. coli* synthesizing MBP, MBP–Dyn2p, MBP–Pex14p, or MBP–Pex17p. Bound proteins, as well as input proteins (2% of load for MBP, MBP–Dyn2p and MBP–Pex14p, and 10% of load for MBP–Pex17p) were analyzed by immunoblotting with anti-MBP antibodies. Total GST and GST-tagged protein levels were visualized by immunoblotting with anti-GST antibodies. (B) Schematic of mutations used to characterize the requirement of amino acids V99DAQTQTE106 of Pex17p for its interaction with Dyn2p. Numbers in the schematic represent the positions of amino acids. (C) The amino acids V99DAQTQTE106 of Pex17p are required for its interaction with Dyn2p. Glutathione–Sepharose beads containing GST–Dyn2p (upper) or GST–Pex14p (lower) were incubated with extracts of *E. coli* synthesizing MBP or MBP fused to the N-terminus of the Pex17p mutations shown in B. Bound proteins, as well as input proteins (10% of all loads), were analyzed by immunoblotting with anti-MBP antibodies. Total GST–Dyn2p and GST–Pex14p levels were visualized by immunoblotting with anti-GST antibodies.

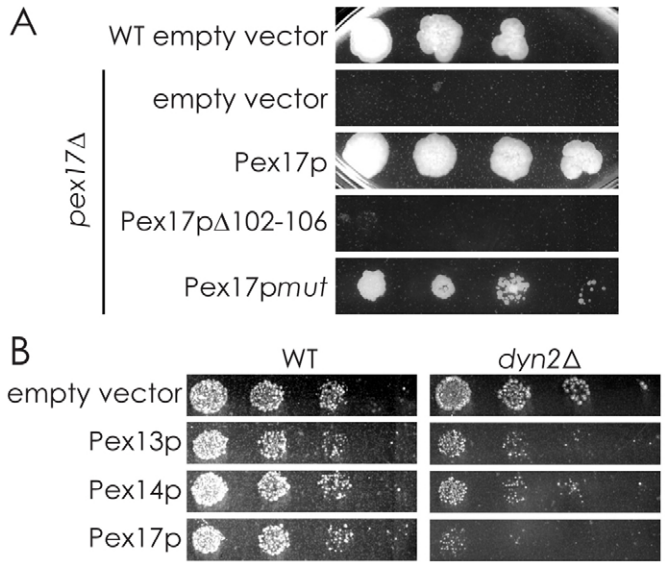

Fig. 7. Growth of strains on oleic-acid-containing medium. (A) Ability of the Pex17p mutations Pex17pΔ102–106 and Pex17p*mut* to restore growth to the *pex17*Δ strain on oleic-acid-containing YPBO medium. (B) Deletion of the *DYN2* gene enhances growth defects on oleic-acid-containing medium because of overexpression of genes encoding the matrix protein import docking complex components Pex13p, Pex14p and Pex17p. Growth on oleic-acid-containing minimal medium, the metabolism of which requires functional peroxisomes, was observed by serial dilution of strains transformed with parental or recombinant pINA445 vector.

YPBO. In contrast, introduction of Pex17pΔ102–106 failed to restore growth of the *pex17*Δ strain on YPBO medium, whereas introduction of Pex17p*mut* led to a weak restoration of growth. The increased severity of the growth defect on YPBO medium of the *pex17*Δ strain expressing Pex17pΔ102–106 as compared with the *dyn2*Δ strain (Fig. 1B) suggests that the amino acids, Q102TQTE106, play a role in Pex17p functionality in addition to their being part of the Pex17p interaction domain with Dyn2p.

We also examined genetic interactions between *DYN2* and the genes coding for the matrix protein import docking complex proteins Pex13p, Pex14p and Pex17p (Fig. 7B). Overexpression of all docking complex genes strongly retarded growth of *dyn2*Δ cells on oleic-acid-containing medium compared with overexpression in wild-type cells. Overexpression of *PEX17* in particular had the strongest effect upon the growth of *dyn2*Δ cells. These results indicate that Dyn2p can mitigate the adverse effects of docking complex gene overexpression.

Discussion

There is increasing evidence that individual components of the microtubule motor dynein have functions not related to transport (Bharti et al., 2011; Fan et al., 1998; Navarro-Lérida et al., 2004; Stelter et al., 2007). *S. cerevisiae* dynein light chain, Dyn2p, was shown to localize in part to peroxisomes through its interaction with Pex14p (Stelter et al., 2007), which, together with Pex13p and Pex17p, forms the receptor docking complex for the import of matrix proteins into the peroxisome (Rucktäschel et al., 2011). The interaction of Dyn2p with Pex14p suggested a role for Dyn2p in peroxisome biogenesis, which was also supported by

the observation that *S. cerevisiae* cells deleted for the *DYN2* gene failed to grow on medium containing oleic acid as the sole carbon source (Smith et al., 2006), the metabolism of which requires functional peroxisomes. In this study, we demonstrate a role for Dyn2p in peroxisome biogenesis in the yeast *Y. lipolytica* and provide evidence that Dyn2p acts together with the peroxisomal matrix protein import receptor docking complex to modulate matrix protein import into peroxisomes and peroxisome maturation.

Y. lipolytica cells deleted for the *DYN2* gene exhibited impaired growth on medium containing oleic acid, and abnormal peroxisome morphology, showing that Dyn2p is required for normal peroxisomal function and biogenesis. However, the impairment in peroxisomal function resulting from deletion of the *DYN2* gene is less than that caused by deletion of bona fide PEX genes such as *PEX14* and *PEX17* encoding components of the peroxisomal matrix protein import docking complex, which are central to the matrix protein import process and are indispensable for peroxisome biogenesis. Therefore, Dyn2p apparently has an auxiliary, rather than a primary, role in peroxisome biogenesis. An auxiliary peroxisome biogenic role for Dyn2p is also supported by our observations that normal peroxisome profiles are sometimes seen in *dyn2*Δ cells by both confocal fluorescence microscopy and electron microscopy, and by the presence of vesicular structures with the biochemical characteristics of wild-type peroxisomes in isopycnic density centrifugation analysis of *dyn2*Δ cells. Dyn2p apparently functions in peroxisome biogenesis primarily under conditions of peroxisome proliferation, because differences in peroxisome structure and matrix protein import between *dyn2*Δ cells and wild-type cells were most evident in cells incubated in oleic-acid-containing medium, in which peroxisome proliferation occurs, and not in medium containing glucose, which does not require peroxisomal activity for its metabolism.

Subcellular fractionation demonstrated that protein targeting to the peroxisomal matrix is compromised in cells deleted for the *DYN2* gene. A comparison of the differential centrifugation fractionation patterns of matrix proteins from wild-type and *dyn2*Δ cells showed that matrix proteins from *dyn2*Δ cells localize to a high-speed supernatant fraction enriched for cytosolic proteins and a high-speed pellet fraction enriched for small vesicles, including peroxisomal vesicles, to a greater degree than matrix proteins from wild-type cells. Protease protection analysis confirmed a defect in matrix protein import in *dyn2*Δ cells. Density gradient centrifugation also showed that the matrix protein composition in fractions of lower buoyant density, normally enriched for small peroxisomal vesicles, differed in extracts from in wild-type and *dyn2*Δ cells. Similarly, matrix proteins from wild-type and *dyn2*Δ cells were differently distributed across fractions of high buoyant density where peroxisomes fractionate. This difference in peroxisome populations between wild-type and *dyn2*Δ cells was also evident by fluorescence microscopy, as the localization patterns of the peroxisomal marker proteins Pot1p–mRFP and, to a lesser extent, mRFP–SKL were different in *dyn2*Δ and wild-type cells. Peroxisomes without their normal complement of matrix proteins might be expected to be only partially functional, which is consistent with our observation that deletion of the *DYN2* gene impairs, but does not eliminate, growth of *Y. lipolytica* cells on fatty-acid-containing medium, the metabolism of which requires peroxisomal activity. Together, our results demonstrate that deletion of the *DYN2* gene results in impaired targeting of matrix proteins to the peroxisome, leading to compromised peroxisome maturation and function during peroxisome proliferation.

The differences in overall composition of the peroxisome populations between wild-type and *dyn2*Δ cells could result from direct influences on the peroxisome biogenic cascade in *Y. lipolytica* brought about by deletion of the *DYN2* gene; however, the physical and genetic interactions between Dyn2p and the components of the peroxisomal matrix protein import docking complex, Pex13p, Pex14p and Pex17p, suggest strongly that the role of Dyn2p in peroxisome biogenesis is related, to a large degree, to its functioning in matrix protein import. Dyn2p could act as a kind of molecular glue at the docking complex, stabilizing protein–protein interactions within a multi-protein complex, similar to the role proposed for *S. cerevisiae* Dyn2p at the nuclear pore in stabilizing the Nup82p–Nsp1p–Nup159p complex (Stelter et al., 2007). Stabilization of the peroxisomal matrix protein import docking complex by Dyn2p could facilitate the import of matrix proteins or perhaps provide a degree of temporal control to peroxisome assembly by determining what matrix proteins are imported at what time. It should also be noted that Dyn2p interacts more strongly with Pex17p than Pex14p in our *in vitro* pull-down assay and that association of Dyn2p with Pex14p in BiFC experiments requires Pex17p. These data suggest that Dyn2p interacts primarily with Pex17p and that its association with Pex14p is due to the close proximity of Pex14p to Pex17p in the matrix protein import docking complex. Since Pex17p functions prior to the formation of the transient import pore (Meinecke et al., 2010), its interactions with Dyn2p and its requirement for interaction with another docking complex component, Pex14p, suggest that Dyn2p may play a stabilizing function early in the formation of the docking complex. Further study will be needed to determine whether this is indeed the case.

In summary, we have shown that *Y. lipolytica* dynein light chain protein, Dyn2p, functions in peroxisome biogenesis. Dyn2p localizes in part to peroxisomes and influences the targeting of proteins to the peroxisomal matrix and, by extension, peroxisome maturation, probably through its interactions with components of the matrix protein import docking complex, especially Pex17p. The role of Dyn2p in peroxisome biogenesis adds to the list of non-motility-related functions that can be attributed to individual components of the dynein motor.

Materials and Methods

Strains and culture conditions

The yeast strains used in this study are listed in supplementary material Table S1. Strains were cultured at 30℃. Strains containing plasmid pTC3 or pINA445 were cultured in minimal medium (YNA or YNO) supplemented with leucine, uracil and lysine, each at 50 μg/ml, as required. Strains containing plasmid pUB4 were cultured in YPA, YPD or YPBO medium supplemented with hygromycin B at 125 μg/ml. Media components were as follows: YNA, 0.67% yeast nitrogen base without amino acids, 2% sodium acetate; YNO, 0.67% yeast nitrogen base without amino acids, 0.05% Tween 40, 0.1% oleic acid; YPA, 1% yeast extract, 2% peptone, 2% sodium acetate; YPD, 1% yeast extract, 2% peptone, 2% glucose; YPG, 1% yeast extract, 2% peptone, 2% glycerol; YPBO, 0.3% yeast extract, 0.5% peptone, 0.5% K_2HPO_4, 0.5% KH_2PO_4, 1% Brij 35, 1% oleic acid.

Integrative gene disruption

Genes were disrupted by homologous transformation using fusion PCR-based integration (Davidson et al., 2002).

Plasmids

pINA445 (Nuttley et al., 1993), pTC3 (Lin et al., 1999) and pUB4 (Kerscher et al., 2001) have been described. DNA encoding mRFP–SKL and flanked by promoter

and terminator sequences of the *POT1* gene was amplified by PCR from pTC3-mRFP-SKL (Chang et al., 2007) and inserted at the *Cla*I site of pINA445 and pUB4 to produce pINA445-mRFP-SKL and pUB4-mRFP-SKL. DNA encoding Pex13p, Pex14p and Pex17p, and GFP-N (amino acids 1–156 of GFP) and GFP-C (amino acids 157–238 of GFP) used for bimolecular fluorescence complementation (split GFP) analysis, was amplified by PCR. The chimeric genes encoding Pot1p–mRFP, Dyn2p–mCherry, Dyn2p–GFP-N and Pex14p–GFP-C, and the genes encoding Pex17p*mut* and Pex17pΔ102–106, were constructed by fusion PCR. PCR products were inserted into the *Eco*RI site of pTC3 to make pTC3-POT1-mRFP, pTC3-GFP-N, pTC3-GFP-C, pTC3-DYN2, pTC3-DYN2-mCherry, pTC3-DYN2-GFP-N, pTC3-PEX14-GFP-C, pTC3-PEX13, pTC3-PEX14, pTC3-PEX17, pTC3-PEX17*mut* and pTC3-PEX17Δ102–106. pUB4-POT1-mRFP, pUB4-GFP-C, pUB4-DYN2, pUB4-DYN2-mCherry, pUB4-DYN2-GFP-N and pUB4-PEX14-GFP-C were made similarly to pUB4-mRFP-SKL. pINA445-PEX13, pINA445-PEX14 and pINA445-PEX17 were made similarly to pINA445-mRFP-SKL.

Microscopy

Fluorescence images were captured with a LCI Plan-Neofluar 63×/1.3 NA objective on an Axiovert 200 microscope equipped with a LSM510 META confocal scanner (Carl Zeiss). Stacks of 3 (Fig. 2) or 21 (Fig. 5) optical sections each spaced 1 or 0.25 μm apart were captured. Acquired images were processed as described previously (Tower et al., 2011). To remove blur, experimentally generated three-dimensional (3D) data sets were deconvolved through an iterative classic maximum likelihood estimation algorithm and an experimentally derived point spread function using Huygens Professional software (Scientific Volume Imaging, Hilversum, The Netherlands). Imaris 7.3 software (Bitplane) was used to prepare maximum intensity, or 'Blend-view', projections of deconvolved 3D data sets. Projections were used to generate single images. Transmission images were treated with a Gaussian filter and made white in Imaris. Collections of images were assembled into figures using Adobe Photoshop CS4 and Adobe Illustrator CS4 (Adobe Systems). Electron microscopy of whole yeast cells was performed as described previously (Eitzen et al., 1997).

Cell fractionation and peroxisome subfractionation

Wild-type and *dyn2*Δ cells were cultured in YPD or YPBO medium. *dyn2*Δ cells transformed with pUB4-DYN2-mCherry were cultured in YPD medium supplemented with hygromycin B. Cell fractionation was performed essentially as described previously (Szilard et al., 1995). Homogenized spheroplasts were subjected to differential centrifugation at 1000 ***g*** for 10 minutes at 4℃ in a JS13.1 rotor (Beckman) to yield a postnuclear supernatant (PNS) fraction. The PNS fraction was subjected to differential centrifugation at 20,000 ***g*** for 30 minutes at 4℃ to yield a pellet (20KgP) fraction enriched for peroxisomes and mitochondria, and a supernatant (20KgS) fraction enriched for cytosol and high-speed pelletable organelles. The 20KgS fraction was further subjected to differential centrifugation at 200,000 ***g*** for 1 hour at 4℃ in a TLA120.2 rotor (Beckman) to yield a pellet (200KgP) fraction enriched for high-speed pelletable organelles including small peroxisomal vesicles, and a supernatant (200KgS) fraction enriched for cytosol.

Peroxisomes were purified from the 20KgP fraction by isopycnic centrifugation on a discontinuous Nycodenz gradient at 100,000 ***g*** for 90 minutes in a VTi50 rotor (Beckman) (Titorenko et al., 1996). 20KgP and 200KgP fractions were treated with dilute alkali Tris buffer and separated into fractions enriched for matrix and membrane proteins by ultracentrifugation as described previously (Vizeacoumar et al., 2003).

Assay for direct protein binding

Fusions of GST to Dyn2p, Pex14p and Pex17p were constructed using pGEX4T-1 (GE Healthcare). Recombinant expression and immobilization of GST, GST–Dyn2p, GST–Pex14p and GST–Pex17p on glutathione–Sepharose resin were performed according to the manufacturer's instructions. MBP fusions to Dyn2p, Pex14p, Pex17p and Pex17p mutations were constructed using pMAL-c2 (New England Biolabs) and expressed in *E. coli* strain BL21 (Invitrogen). 250 μg of purified GST, GST–Dyn2p, GST–Pex14p or GST–Pex17p immobilized on glutathione–Sepharose resin were incubated with 250 μg of *E. coli* lysate containing MBP or MBP fusion protein (50 μg for MBP–Pex17p and MBP–Pex17p mutations) in PBS buffer containing 0.5% Triton X-100 and 2× complete protease inhibitor (Roche) for 3 hours at 4℃ on a rocking platform. After settling, the resin was washed five times with PBS buffer containing 0.5% Triton X-100. Immobilized proteins were eluted by boiling in sample buffer and subjected to SDS-PAGE and immunoblotting.

Antibodies

Antibodies to Pot1p, Sdh2p, Aox1p, Aox3p, Aox5p, MLS, SKL, ICL, Pex2p, Pex3Bp, Pex19p, DsRed and GST have been described previously (Chang et al., 2009; Lambkin and Rachubinski, 2001; Titorenko et al., 2000; 2002). Mouse anti-MBP monoclonal antibody was from New England Biolabs. For immunoblot analysis, HRP-conjugated donkey anti-rabbit IgG, HRP-conjugated goat anti-guinea pig IgG, and HRP-conjugated sheep anti-mouse IgG secondary antibodies were used to detect primary antibodies, and antigen–antibody complexes were detected by enhanced chemiluminescence (GE Healthcare).

Acknowledgements

We thank Richard Poirier, Elena Savidov, Hanna Kroliczak and Dwayne Weber for expert technical assistance and members of the Rachubinski laboratory for helpful discussions. R.A.R. is an International Research Scholar of the Howard Hughes Medical Institute.

Author contributions

J.C., R.J.T., D.L.L. and R.A.R. provided a conceptual framework for the study, interpreted data and wrote the manuscript. J.C. and R.J.T. performed the experiments.

Funding

This work was supported by the Howard Hughes Medical Institute [grant number 55005958 to R.A.R.]; and the Canadian Institutes of Health [grant number 9208 to R.A.R.]. Deposited in PMC for release after 6 months.

Supplementary material available online at
http://jcs.biologists.org/lookup/suppl/doi:10.1242/jcs.129056/-/DC1

References

Berg, R. K., Melchjorsen, J., Rintahaka, J., Diget, E., Søby, S., Horan, K. A., Gorelick, R. J., Matikainen, S., Larsen, C. S., Ostergaard, L. et al. (2012). Genomic HIV RNA induces innate immune responses through RIG-I-dependent sensing of secondary-structured RNA. *PLoS ONE* **7**, e29291.

Bharti, P., Schliebs, W., Schievelbusch, T., Neuhaus, A., David, C., Kock, K., Herrmann, C., Meyer, H. E., Wiese, S., Warscheid, B. et al. (2011). PEX14 is required for microtubule-based peroxisome motility in human cells. *J. Cell Sci.* **124**, 1759-1768.

Chang, J., Fagarasanu, A. and Rachubinski, R. A. (2007). Peroxisomal peripheral membrane protein Ylnp1p is required for peroxisome inheritance and influences the dimorphic transition in the yeast Yarrowia lipolytica. *Eukaryot. Cell* **6**, 1528-1537.

Chang, J., Mast, F. D., Fagarasanu, A., Rachubinski, D. A., Eitzen, G. A., Dacks, J. B. and Rachubinski, R. A. (2009). Pex3 peroxisome biogenesis proteins function in peroxisome inheritance as class V myosin receptors. *J. Cell Biol.* **187**, 233-246.

Davidson, R. C., Blankenship, J. R., Kraus, P. R., de Jesus Berrios, M., Hull, C. M., D'Souza, C., Wang, P. and Heitman, J. (2002). A PCR-based strategy to generate integrative targeting alleles with large regions of homology. *Microbiology* **148**, 2607-2615.

Dixit, E., Boulant, S., Zhang, Y., Lee, A. S. Y., Odendall, C., Shum, B., Hacohen, N., Chen, Z. J., Whelan, S. P., Fransen, M. et al. (2010). Peroxisomes are signaling platforms for antiviral innate immunity. *Cell* **141**, 668-681.

Eitzen, G. A., Szilard, R. K. and Rachubinski, R. A. (1997). Enlarged peroxisomes are present in oleic acid-grown Yarrowia lipolytica overexpressing the PEX16 gene encoding an intraperoxisomal peripheral membrane peroxin. *J. Cell Biol.* **137**, 1265-1278.

Fan, J. S., Zhang, Q., Li, M., Tochio, H., Yamazaki, T., Shimizu, M. and Zhang, M. (1998). Protein inhibitor of neuronal nitric-oxide synthase, PIN, binds to a 17-amino acid residue fragment of the enzyme. *J. Biol. Chem.* **273**, 33472-33481.

Fidaleo, M. (2010). Peroxisomes and peroxisomal disorders: the main facts. *Exp. Toxicol. Pathol.* **62**, 615-625.

Giaever, G., Chu, A. M., Ni, L., Connelly, C., Riles, L., Véronneau, S., Dow, S., Lucau-Danila, A., Anderson, K., André, B. et al. (2002). Functional profiling of the Saccharomyces cerevisiae genome. *Nature* **418**, 387-391.

Gould, S. J., Keller, G. A., Hosken, N., Wilkinson, J. and Subramani, S. (1989). A conserved tripeptide sorts proteins to peroxisomes. *J. Cell Biol.* **108**, 1657-1664.

Hoepfner, D., Schildknegt, D., Braakman, I., Philippsen, P. and Tabak, H. F. (2005). Contribution of the endoplasmic reticulum to peroxisome formation. *Cell* **122**, 85-95.

Horner, S. M., Liu, H. M., Park, H. S., Briley, J. and Gale, M., Jr (2011). Mitochondrial-associated endoplasmic reticulum membranes (MAM) form innate immune synapses and are targeted by hepatitis C virus. *Proc. Natl. Acad. Sci. USA* **108**, 14590-14595.

Islinger, M., Cardoso, M. J. R. and Schrader, M. (2010). Be different—the diversity of peroxisomes in the animal kingdom. *Biochim. Biophys. Acta* **1803**, 881-897.

Kardon, J. R. and Vale, R. D. (2009). Regulators of the cytoplasmic dynein motor. *Nat. Rev. Mol. Cell Biol.* **10**, 854-865.

Kerscher, S. J., Eschemann, A., Okun, P. M. and Brandt, U. (2001). External alternative NADH:ubiquinone oxidoreductase redirected to the internal face of the mitochondrial inner membrane rescues complex I deficiency in Yarrowia lipolytica. *J. Cell Sci.* **114**, 3915-3921.

Kim, P. K., Mullen, R. T., Schumann, U. and Lippincott-Schwartz, J. (2006). The origin and maintenance of mammalian peroxisomes involves a de novo PEX16-dependent pathway from the ER. *J. Cell Biol.* **173**, 521-532.

Lambkin, G. R. and Rachubinski, R. A. (2001). Yarrowia lipolytica cells mutant for the peroxisomal peroxin Pex19p contain structures resembling wild-type peroxisomes. *Mol. Biol. Cell* **12**, 3353-3364.

Lin, Y., Sun, L., Nguyen, L. V., Rachubinski, R. A. and Goodman, H. M. (1999). The Pex16p homolog SSE1 and storage organelle formation in Arabidopsis seeds. *Science* **284**, 328-330.

Ma, C., Agrawal, G. and Subramani, S. (2011). Peroxisome assembly: matrix and membrane protein biogenesis. *J. Cell Biol.* **193**, 7-16.

Marzioch, M., Erdmann, R., Veenhuis, M. and Kunau, W. H. (1994). PAS7 encodes a novel yeast member of the WD-40 protein family essential for import of 3-oxoacyl-CoA thiolase, a PTS2-containing protein, into peroxisomes. *EMBO J.* **13**, 4908-4918.

Mast, F. D., Fagarasanu, A., Knoblach, B. and Rachubinski, R. A. (2010). Peroxisome biogenesis: something old, something new, something borrowed. *Physiology (Bethesda)* **25**, 347-356.

Mauersberger, S., Wang, H. J., Gaillardin, C., Barth, G. and Nicaud, J. M. (2001). Insertional mutagenesis in the n-alkane-assimilating yeast Yarrowia lipolytica: generation of tagged mutations in genes involved in hydrophobic substrate utilization. *J. Bacteriol.* **183**, 5102-5109.

McCollum, D., Monosov, E. and Subramani, S. (1993). The pas8 mutant of Pichia pastoris exhibits the peroxisomal protein import deficiencies of Zellweger syndrome cells—the PAS8 protein binds to the COOH-terminal tripeptide peroxisomal targeting signal, and is a member of the TPR protein family. *J. Cell Biol.* **121**, 761-774.

Meinecke, M., Cizmowski, C., Schliebs, W., Krüger, V., Beck, S., Wagner, R. and Erdmann, R. (2010). The peroxisomal importomer constitutes a large and highly dynamic pore. *Nat. Cell Biol.* **12**, 273-277.

Moore, J. K., Stuchell-Brereton, M. D. and Cooper, J. A. (2009). Function of dynein in budding yeast: mitotic spindle positioning in a polarized cell. *Cell Motil. Cytoskeleton* **66**, 546-555.

Motley, A. M. and Hettema, E. H. (2007). Yeast peroxisomes multiply by growth and division. *J. Cell Biol.* **178**, 399-410.

Munck, J. M., Motley, A. M., Nuttall, J. M. and Hettema, E. H. (2009). A dual function for Pex3p in peroxisome formation and inheritance. *J. Cell Biol.* **187**, 463-471.

Navarro-Lérida, I., Martínez Moreno, M., Roncal, F., Gavilanes, F., Albar, J. P. and Rodríguez-Crespo, I. (2004). Proteomic identification of brain proteins that interact with dynein light chain LC8. *Proteomics* **4**, 339-346.

Nuttley, W. M., Brade, A. M., Gaillardin, C., Eitzen, G. A., Glover, J. R., Aitchison, J. D. and Rachubinski, R. A. (1993). Rapid identification and characterization of peroxisomal assembly mutants in Yarrowia lipolytica. *Yeast* **9**, 507-517.

Rucktäschel, R., Girzalsky, W. and Erdmann, R. (2011). Protein import machineries of peroxisomes. *Biochim. Biophys. Acta* **1808**, 892-900.

Schrader, M., Bonekamp, N. A. and Islinger, M. (2012). Fission and proliferation of peroxisomes. *Biochim. Biophys. Acta* **1822**, 1343-1357.

Smith, J. J., Sydorskyy, Y., Marelli, M., Hwang, D., Bolouri, H., Rachubinski, R. A. and Aitchison, J. D. (2006). Expression and functional profiling reveal distinct gene classes involved in fatty acid metabolism. *Mol. Syst. Biol.* **2**, 0009.

Song, C., Wen, W., Rayala, S. K., Chen, M., Ma, J., Zhang, M. and Kumar, R. (2008). Serine 88 phosphorylation of the 8-kDa dynein light chain 1 is a molecular switch for its dimerization status and functions. *J. Biol. Chem.* **283**, 4004-4013.

Steinberg, S. J., Dodt, G., Raymond, G. V., Braverman, N. E., Moser, A. B. and Moser, H. W. (2006). Peroxisome biogenesis disorders. *Biochim. Biophys. Acta* **1763**, 1733-1748.

Stelter, P., Kunze, R., Flemming, D., Höpfner, D., Diepholz, M., Philippsen, P., Böttcher, B. and Hurt, E. (2007). Molecular basis for the functional interaction of dynein light chain with the nuclear-pore complex. *Nat. Cell Biol.* **9**, 788-796.

Stuchell-Brereton, M. D., Siglin, A., Li, J., Moore, J. K., Ahmed, S., Williams, J. C. and Cooper, J. A. (2011). Functional interaction between dynein light chain and intermediate chain is required for mitotic spindle positioning. *Mol. Biol. Cell* **22**, 2690-2701.

Swinkels, B. W., Gould, S. J., Bodnar, A. G., Rachubinski, R. A. and Subramani, S. (1991). A novel, cleavable peroxisomal targeting signal at the amino-terminus of the rat 3-ketoacyl-CoA thiolase. *EMBO J.* **10**, 3255-3262.

Szilard, R. K., Titorenko, V. I., Veenhuis, M. and Rachubinski, R. A. (1995). Pay32p of the yeast Yarrowia lipolytica is an intraperoxisomal component of the matrix protein translocation machinery. *J. Cell Biol.* **131**, 1453-1469.

Tabak, H. F., van der Zand, A. and Braakman, I. (2008). Peroxisomes: minted by the ER. *Curr. Opin. Cell Biol.* **20**, 393-400.

Titorenko, V. I. and Rachubinski, R. A. (2000). Peroxisomal membrane fusion requires two AAA family ATPases, Pex1p and Pex6p. *J. Cell Biol.* **150**, 881-886.

Titorenko, V. I. and Rachubinski, R. A. (2001). The life cycle of the peroxisome. *Nat. Rev. Mol. Cell Biol.* **2**, 357-368.

Titorenko, V. I., Eitzen, G. A. and Rachubinski, R. A. (1996). Mutations in the PAY5 gene of the yeast Yarrowia lipolytica cause the accumulation of multiple subpopulations of peroxisomes. *J. Biol. Chem.* **271**, 20307-20314.

Titorenko, V. I., Chan, H. and Rachubinski, R. A. (2000). Fusion of small peroxisomal vesicles in vitro reconstructs an early step in the in vivo multistep peroxisome assembly pathway of Yarrowia lipolytica. *J. Cell Biol.* **148**, 29-44.

Titorenko, V. I., Nicaud, J. M., Wang, H., Chan, H. and Rachubinski, R. A. (2002). Acyl-CoA oxidase is imported as a heteropentameric, cofactor-containing complex into peroxisomes of Yarrowia lipolytica. *J. Cell Biol.* **156**, 481-494.

Tower, R. J., Fagarasanu, A., Aitchison, J. D. and Rachubinski, R. A. (2011). The peroxin Pex34p functions with the Pex11 family of peroxisomal divisional proteins to regulate the peroxisome population in yeast. *Mol. Biol. Cell* **22**, 1727-1738.

van der Zand, A., Gent, J., Braakman, I. and Tabak, H. F. (2012). Biochemically distinct vesicles from the endoplasmic reticulum fuse to form peroxisomes. *Cell* **149**, 397-409.

Vizeacoumar, F. J., Torres-Guzman, J. C., Tam, Y. Y. C., Aitchison, J. D. and Rachubinski, R. A. (2003). YHR150w and YDR479c encode peroxisomal integral membrane proteins involved in the regulation of peroxisome number, size, and distribution in Saccharomyces cerevisiae. *J. Cell Biol.* **161**, 321-332.